2004

Formation and properties of halogenated aluminum clusters

D. E. Bergeron
The Pennsylvania State University

A. W. Castleman Jr.
The Pennsylvania State University

T. Morisato
Virginia Commonwealth University

S. N. Khanna
Virginia Commonwealth University

Bergeron, D. E., Castleman, A. W., Morisato, T., et al. Formation and properties of halogenated aluminum clusters. The Journal of Chemical Physics 121, 10456 (2004). Copyright © 2004 AIP Publishing LLC.

Formation and properties of halogenated aluminum clusters

D. E. Bergeron and A. W. Castleman, Jr.[a)]
Departments of Chemistry and Physics, The Pennsylvania State University, University Park, Pennsylvania 16802

T. Morisato and S. N. Khanna
Department of Physics, Virginia Commonwealth University, Richmond, Virginia 23284-2000

(Received 23 July 2004; accepted 23 August 2004)

The fast-flow tube reaction apparatus was employed to study the halogenation of aluminum clusters. For reactions with HX (X=Cl, Br, and I), acid-etching pathways are evident, and we present findings for several reactions, whereby Al_nX^- generation is energetically favorable. Tandem reaction experiments allowed us to establish that for Al_nCl^-, Al_nI^-, and $Al_nI_2^-$, species with $n=6$, 7, and 15 are particularly resistant to attack by oxygen. Further, trends in reactivity suggest that, in general, iodine incorporation leaves the aluminum clusters' electronic properties largely unperturbed. *Ab initio* calculations were performed to better interpret reaction mechanisms and elucidate the characteristics of the products. Lowest energy structures for $Al_{13}X^-$ were found to feature icosahedral Al_{13} units with the halogen atom located at the on-top site. The charge density of the highest occupied molecular orbital in these clusters is heavily dependent on the identity of X. The dependence of reactivity on the clusters' charge state is also discussed. In addition, we address the enhanced stability of $Al_{13}I^-$ and $Al_{13}I_2^-$, arguing that the superhalogen behavior of Al_{13} in these clusters can provide unique opportunities for the synthesis of novel materials with saltlike structures.
 [DOI: 10.1063/1.1806416]

I. INTRODUCTION

The Jellium description[1] provides a simplistic yet generally reliable model for the prediction of magic numbers in many metallic cluster systems, aluminum being a notable example.[2,3] Due to the simultaneous occurrence of several geometric and electronic shell closings, aluminum clusters have received substantial theoretical attention, holding a prominent position in the literature surrounding the assembly of superatomic cluster-based materials. Theoretical predictions of superatomic salt formation[4–7] have fueled much research in this area, and with increasing frequency, various synthetic techniques have been applied to the realization of aluminum-based cluster-assembled materials.[8–10] While many studies involving the doping of Al clusters with electropositive atoms have supported the conceptual basis for superatomic cluster assembly,[11–17] no true saltlike materials have yet been built from bare clusters mimicking atoms. The utilization of superatoms in materials synthesis will ultimately provide a third dimension to the traditional periodic table of elements, representing an entirely new generation of nanostructured materials.

Recently, we reported on the neutralization of Al_n^- clusters via reaction with methyl iodide (MeI) to form Al_nCH_3.[18] The interaction between the cluster and the methyl group was shown to be covalent in nature, and by comparison with boron reactions,[19] we proposed that the formation of the cluster-CH_3 bond was site specific, very likely effecting an interruption in the clusters' electron delocalization. In addition, we have recently performed tandem reaction experiments,[20] discovering that the magic aluminum clusters, Al_{13}^- and Al_{23}^-, do not participate appreciably in a reaction with MeI.

Study of the reaction between Al_n^- and MeI also led us to the discovery of a series of Al_nI^- clusters occurring as a "side product." We have since studied the occurrence of a magic cluster anion containing 13 aluminum atoms and 1 iodine atom.[21] The cluster forms readily in the reaction between aluminum clusters and HI, and its predominance is attributed partially to the resistance of Al_{13}^- to acid etching. As both Al_{13}^- and I^- have closed electronic shells, and due to the fact that aluminum and iodine readily react to form covalent molecules, the discovery of the supermagic $Al_{13}I^-$ was quite unexpected. We believe that the electronic structure of this cluster may prove instructive in the design of future saltlike cluster assembled materials.

In the present study, we offer a much more comprehensive view of aluminum cluster halogenation. Experiments designed to shed more light on the reaction pathways at work are presented. Reactions with HCl and HBr are also described and are compared to the results obtained with HI and MeI. While acid etching played a major role in the previously reported reaction of Al_n^- with HI, we show that this pathway is far less favorable for the HCl and HBr cases. Still, some chemical similarities are observed and are addressed herein. The role of increasing electron affinity (EA) upon ascension of the periodic table is considered, but we show that the most important factor in the reactions presented is related to H–X (X=Cl, Br, and I) bond strength.

In no case do the reactions of Al_n^- with HX yield appreciable X^- as a product, so the type of reaction observed for

[a)]Electronic mail: awc@psu.edu

the MeI case is notably absent. We describe several of the reactions that we believe to be key in the current work, including energetic evaluations derived from known values and *ab initio* treatments of the clusters under consideration.

Theoretical electronic structure calculations have been carried out to aid in the interpretation of the experimental findings. The basic questions addressed by these calculations include: (1) Why does HI etch the Al_n^- clusters more efficiently than HBr or HCl? This is particularly surprising since the experimental binding energy of AlCl is 5.2 eV as compared to 3.8 eV for AlI. (2) Why do Al_nI^- ($n=6$, 7, 13, and 15) emerge as magic species in oxygen-etching experiments? (3) Since Al_7^- and Al_{13}^- have been seen as magic clusters in past experiments, might the Al_7I^- and $Al_{13}I^-$ clusters form by a mere fragmentation of HI and attachment of I to the nascent clusters, or is there a new mechanism for their formation? (4) Why does $Al_{13}Cl^-$ form so reluctantly and react so readily with oxygen, whereas $Al_{13}I^-$ forms facilely and represents a favored product in oxygen-etching experiments? What are the electronic structures of these seemingly similar species, and how is the ''extra'' electron of the anion shared between the Al_{13} moiety and the halogen atoms? To answer these questions, we carried out first-principles density-functional calculations on neutral and anionic $Al_{13}X$ (X=H, I, and Cl), $Al_{13}I_2$, and on some of the dimers involving Al, H, I, and Cl. These investigations, combined with some of our earlier work on pure Al_n^- ($n=12-14$),[22] allowed us to elucidate the mechanisms underlying the etching of pure clusters, as well as the electronic nature of $Al_{13}X$ (X=I and Cl) and $Al_{13}I_2$.

Section II is dedicated to the details of the experimental setup, whereas Sec. III gives the details of the theoretical computations. Section IV presents the experimental findings and Sec. V presents the theoretical results. Section VI contains a general discussion of the results, and in Sec. VII, the final conclusions are drawn.

II. EXPERIMENT

The fast-flow tube reaction apparatus employed in the current experiments has been described in detail elsewhere[23] and is only briefly discussed here. Aluminum clusters are generated via laser ablation of a translating and rotating aluminum rod in the presence of a constant flow [8000 standard cubic centimeters per minute (SCCM)] of high-purity helium. The carrier gas effects collisional cooling and cluster formation, passing through a conical nozzle into the flow tube. The flow tube pressure (0.30–0.33 torr) is maintained by a high-volume Roots pump. In experiments where only one reactant gas is introduced, a flow-controlled reactant gas inlet (RGI) of the radial type, located downstream from the source, was employed. In reactions where two reactant gases were introduced, a finger inlet was attached to the ''Y'' branch of the apparatus; this allowed the thermalized clusters to be reacted with one gas, travel approximately 15 cm through the flow tube, and be reacted with a second gas. Flow of reactant gas to the finger inlet was controlled with a needle valve, and concentrations were estimated by observing pressure changes in the flow tube. Upschulte *et al.* have addressed the characteristics of different types of RGIs in detail.[24]

III. COMPUTATIONAL DETAILS

The theoretical studies were carried out within a gradient-corrected density-functional formalism that uses a linear combination of atomic orbitals-molecular orbitals approach. The wave function of the cluster is formed from a linear combination of atomic orbitals centered at the atomic positions. The atomic orbitals are further expressed as a linear combination of Gaussian functions with exponents determined by nonlinear fitting of free-atom wave functions and supplemented by diffuse functions to provide additional variational freedom. The coefficients of the linear combination are determined by solving the Kohn-Sham equations self-consistently. The results reported here are based on an implementation known as the Naval Research Laboratory Molecular Orbital Library (NRLMOL) developed by Pederson and co-workers.[25,26] In this implementation, the Hamiltonian matrix elements are evaluated via numerical integration over a mesh of points. We have used the gradient-corrected exchange-correlation functional proposed by Perdew *et al.*[27] The basis sets[28] for Al consisted of $6s$, $5p$, and $3d$ functions, for Cl consisted of $6s$, $5p$, and $3d$ functions, for I consisted of $8s$, $7p$, and $5d$ functions, and for H consisted of $4s$, $3p$, and $1d$ functions. These basis sets were supplemented by a d function for Al, Cl, and I and by a d and p functions for H. For details, the reader is referred to earlier papers.[28] All the calculations were carried out at an all-electron level. The geometry optimization was carried out by moving atoms along the direction of forces. The threshold for zero force was set at 10^{-3} a.u./Bohr. Several initial configurations were used in order to prevent getting trapped in local minima of the potential-energy surface. No zero point energies are included.

As I is a heavy element, one has to consider the potential influence of relativistic effects. While it is difficult to carry out fully relativistic calculations on $Al_{13}I$, we did investigate the role of these effects by carrying out density-functional calculations using an effective core potential that includes scalar relativistic corrections for the core. These studies were carried out using the GAUSSIAN 98 code.[29] The exchange-correlation effects were included[30–34] using the Beck's three parameter hybrid functional with Lee, Yang, and Parr correlation functional (B3LYP) including gradient corrections. The basis set consisted of an all-electron 6-311+G* basis set for Al, and a LANL2DZ basis for I.[35]

IV. EXPERIMENTAL RESULTS

A. Reactions of Al_n^- with HX (X=Cl, Br, and I)

1. $Al_n^- + HI$

Some results for the reaction of aluminum clusters with HI have been reported in an earlier disclosure by Bergeron *et al.*[21] For reference purposes, mass spectrometric results are shown in Fig. 1. As mentioned previously, a key mechanism in this reaction appears to involve acid etching and I− addition. In an attempt to better understand the true

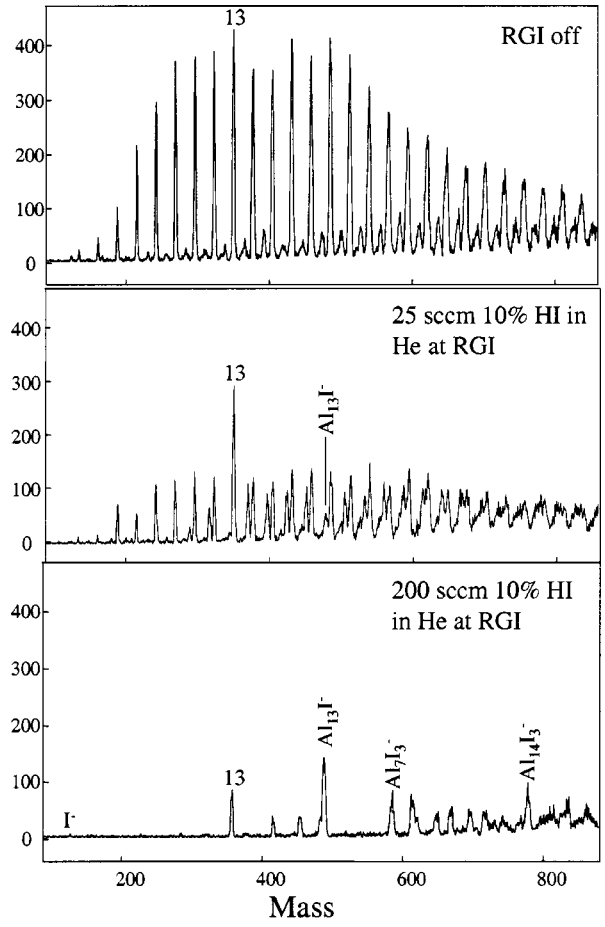

FIG. 1. Mass spectra showing the reaction of Al_n^- with increasing amounts of HI. Reproduced with permission from Ref. 21.

mechanism, an experiment was devised to simulate the HI reaction: aluminum clusters were exposed to MeI (shown previously to generate Al_nI^- clusters when seeded in He)[18] seeded in O_2 (a good etchant for aluminum clusters).[2,3,36] Figure 2 shows the results of this reaction. Excepting the appearance of I^-, the spectra appear exactly as one would expect in the study of O_2 etching of Al clusters. Not only is there a failure to mimic the reaction with HI, which leads to a substantial peak at $Al_{13}I^-$, but there are actually no residual Al_nI^- peaks at all. Clearly, the mechanism of the reaction between Al_n^- and HI is not describable in terms of independent etching and adsorption reactions.

We have also performed experiments in which Al_n^- are subjected to oxygen etching prior to reaction with HI. These studies allow us to specifically monitor the reactions of the magic clusters ($n=13$ and 23). We found that $Al_{13}I^-$ is, in fact, produced in this experiment, indicating that there must be an operative mechanism whereby this species is generated directly from the reaction of Al_{13}^- with HI. In addition, I^- was observed as a product in these experiments. However, as the reaction of oxides of aluminum (products of the etching of Al_n) with HI will exothermically form AlOH and I^-, we do not believe that reaction of Al_{13}^- with HI leads to I^- formation.

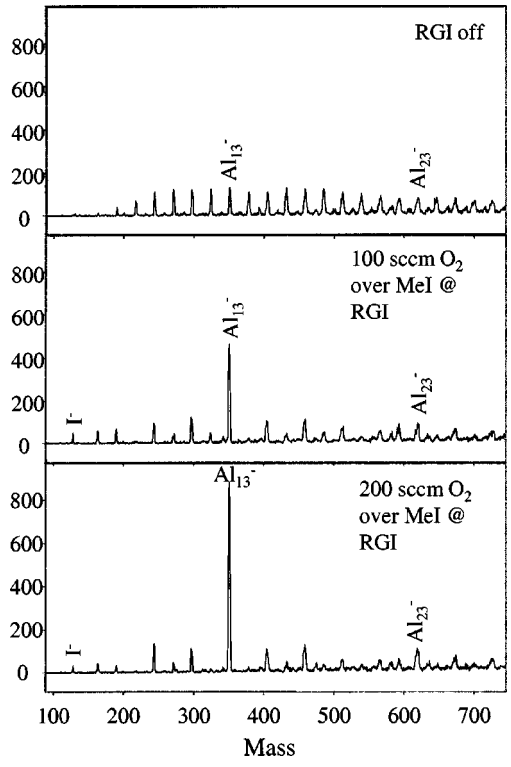

FIG. 2. Mass spectra showing the reaction of Al_n^- with increasing amounts of MeI seeded in O_2.

2. $Al_n^- + HBr$

Figure 3 shows the reaction of aluminum cluster anions with HBr. Several features are immediately evident. Most obviously, the reaction is very different from that observed with HI. We note that even at concentrations as low as 2.5% HI in He, the aluminum cluster distribution disappeared at flow rates of about 150 SCCM, leaving primarily Al_{13}^- and $Al_{13}I^-$. In the presence of over ten times as much HBr, peaks are still present at each initial cluster mass. Several masses are markedly depleted, but the type of dramatic etching seen with HI is not occurring. The most striking depletions occur at Al_{15}^-, Al_{18}^-, Al_{21}^-, Al_{24}^-, and Al_{32}^-. An acid-etching pathway is implicated by the dramatic intensity drops following the closed-shell Jellium clusters, Al_{13}^-, Al_{23}^-, and Al_{37}^-. Two additional drops are observed following Al_{45}^- and Al_{54}^-. While neither of these clusters correspond to Jellium shell closings, Al_{54}^- offers a particular quandary as Al_{55}^- does correspond to a Jellium closing. Experimental and theoretical studies have shown that Al_{55}^- fits the spherical shell model; its geometry is reminiscent of that for Al_{13}^-, and photoelectron spectroscopy has shown that the expected wide highest occupied molecular orbital (HOMO) lowest unoccupied molecular orbital (LUMO) gap is indeed present.[37–39] Therefore, one would expect the intensity drop to follow Al_{55}^-, not Al_{54}^-. As mass degeneracies make the identification of any Br-containing clusters extremely difficult to discern from the Al_n^- series (peak widening due to the two isotopes of Br is clearly evident), we suspect that the magic peak at Al_{54}^- actually corresponds to an $Al_{54-3x}Br_x^-$ cluster. Oxygen-etching experiments (Fig. 4) support this assertion in that no magic peak is observed at Al_{54}^-. In addition, experiments were per-

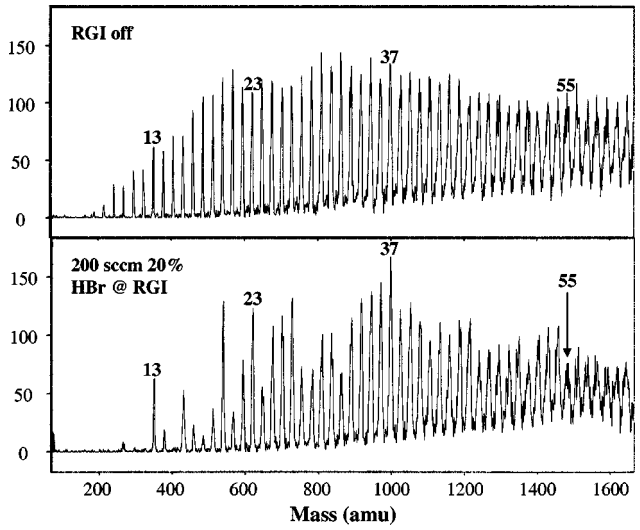

FIG. 3. Mass spectra showing the reaction of Al_n^- with HBr. Mass degeneracies prohibit the identification of Al_nBr^-.

formed in which the ablation laser's power was increased in order to impart the clusters with additional internal energy, thus potentially increasing fragmentation; in this manner, the cluster distribution was ''pushed'' to lower masses. Even when the Al_{54}^- cluster was absent from the reactant distribution, it (and many other high-mass clusters) appeared when the clusters were reacted with HBr. We also suspect that the magic peaks at Al_n^- ($n=20$, 27, and 45) represent brominated clusters ($Al_{n-3x}Br_x^-$).

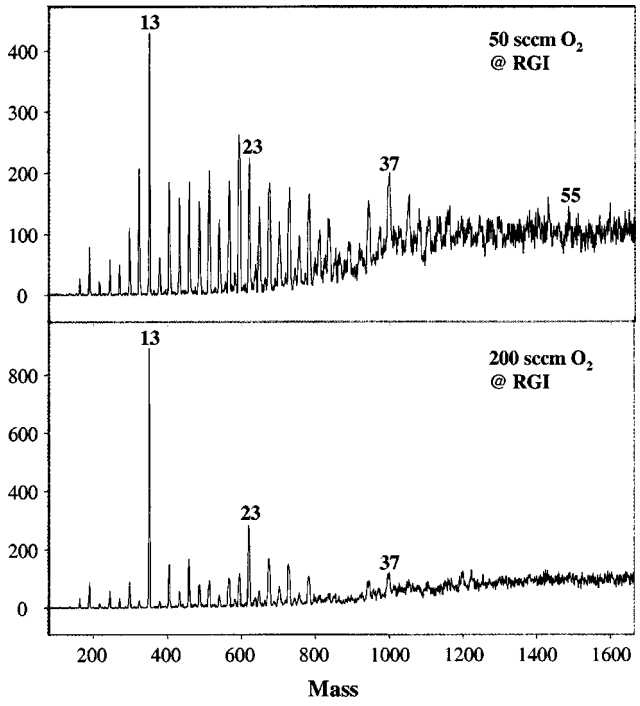

FIG. 4. Mass spectra showing the oxygen etching of Al_n^- by O_2. Only product spectra are shown; the initial cluster distribution resembled that are shown in Fig. 2. Note that very few high-mass clusters survive the etching process, suggesting that the ''Al_{54}^-'' peak in Fig. 2 actually corresponds to the $Al_{54-3x}Br_x^-$ species.

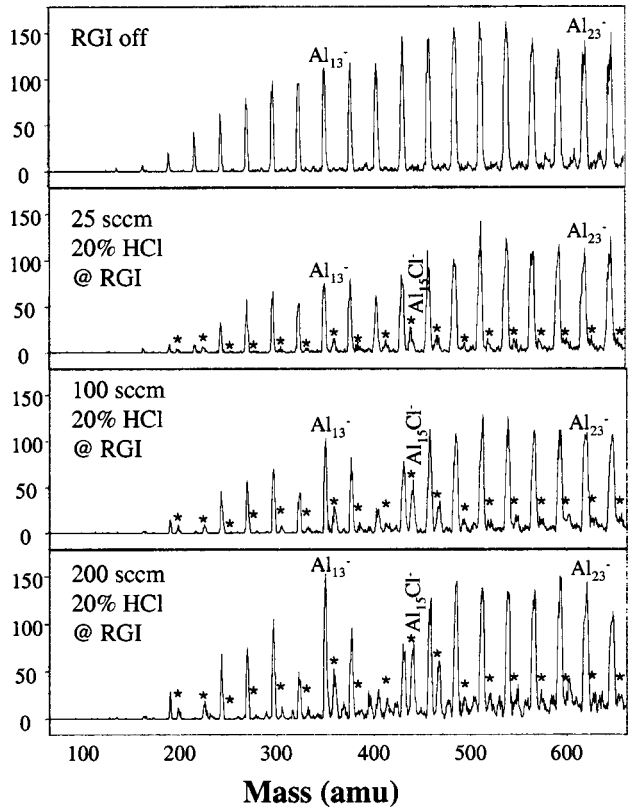

FIG. 5. Mass spectra showing the reaction of Al_n with increasing amounts of HCl. The asterisks mark peaks corresponding to Al_nCl^-.

Although these mass degeneracies make definitive statements very difficult, it is worthwhile to examine the distribution at the masses that would correspond to Al_nBr^- ($n=6$, 7, 13 and 15), as we have observed magic peaks corresponding to these stoichiometries in the reactions with HI. It is possible that the surviving peak at Al_{10}^- in the product distribution is actually Al_7Br^-. More importantly, Al_{16}^-, which does not persist in the oxygen-etching experiments, has an intensity nearly as high as Al_{13}^- in the HBr etching experiment. This peak could, of course, owe at least some of its intensity to $Al_{13}Br^-$. However, Al_{18}^-, which might correspond to $Al_{15}Br^-$, shows no special intensity. While it is difficult to assess to what degree Br-containing clusters contribute to the intensity of any given peak, it is still quite clear that the reaction with HBr is far less dramatic than the reaction with HI.

Martin and Diefenbach[40] have studied aluminum bromide clusters in the past. However, their technique, which featured the evaporation of $AlBr_3$ and electron-impact ionization, led to cationic clusters far more Br rich than would be expected in the present experiments. Not surprisingly, then, our mass spectra do not resemble those of Martin and Diefenbach,[40] and we cannot relate any of the unidentified magic peaks in our experiments to peaks in their distributions.

3. $Al_n^- + HCl$

As shown in Fig. 5, HCl attacks the aluminum cluster anions even more weakly than HBr. The only dramatic

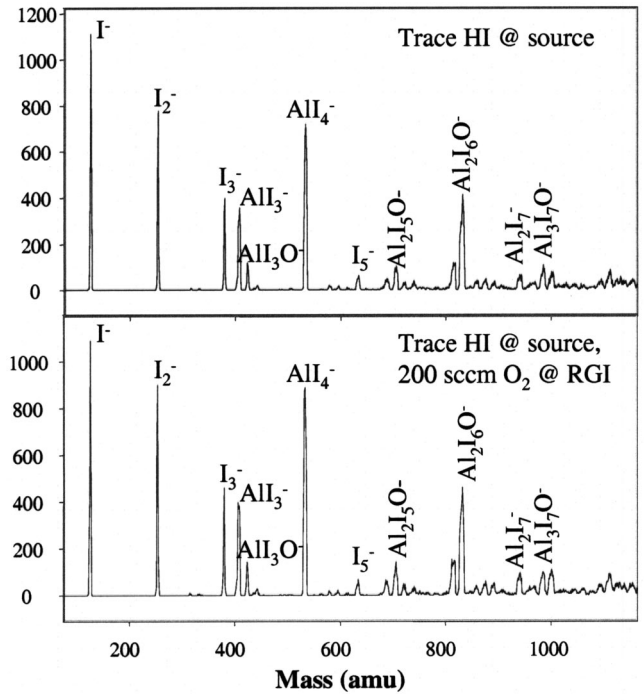

FIG. 6. Mass spectra showing the cluster distribution obtained by passing trace HI over the Al rod in the constant flow LaVa source. The I-rich species produced in this manner are resistant to oxygen etching.

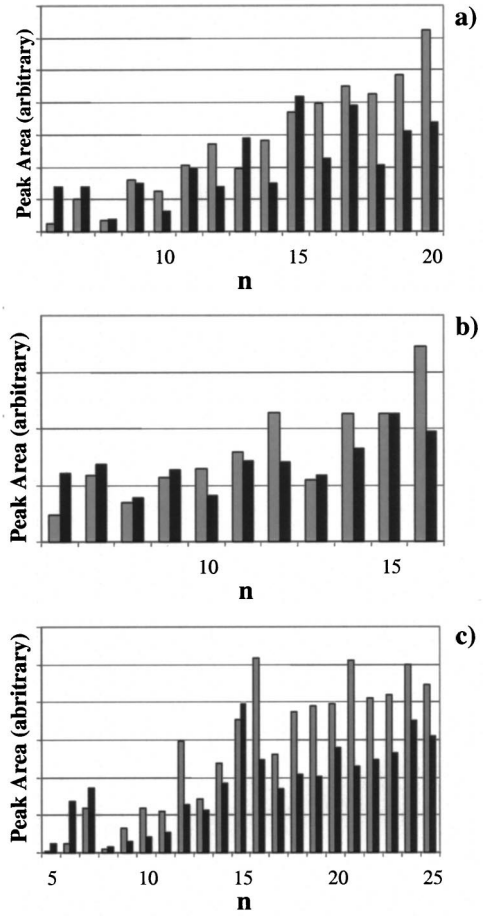

FIG. 7. Integrated peak intensities for (a) Al_nI^-, (b) $Al_nI_2^-$, and (c) Al_nCl^- clusters. Shaded gray are the peak intensities extracted from spectra when small amounts of HX are flowing through the instrument's first RGI with the O_2 RGI off. Shaded black are the peak intensities resulting when the products of the initial reaction with HX are exposed to 200 SCCM of O_2 at the instrument's second RGI.

change in the bare aluminum cluster distribution occurs at Al_{15}^-. This peak disappears upon progressive reactant addition. Interestingly, Al_{15}^- is known to be relatively resistant to etching by O_2.[2] The mass window examined here is much narrower than that shown for HBr; indeed, higher mass ranges were not studied because nothing very interesting was observed to occur beyond the depletion of Al_{15}^-. Easily distinguishable from the bare aluminum clusters are the chlorinated species. Again, when compared to the reaction with HI, more than ten times as much HCl had to be introduced in order to yield even a relatively minimal effect.

B. Determination of Al_nX^- relative stabilities via oxygen etching

A common method for the synthesis of binary clusters involves the dehydrogenation of H-containing gases.[41] As shown in Fig. 6, the synthesis of singly halogenated aluminum clusters via dehydrogenation of HX gases is not possible in the constant flow laser vaporization (LaVa) source, likely due to a suppression of Al incorporation caused by the presence of HI in the laser-induced plasma. In the HI case, passing the hydrogen halide through the laser-plasma source region yielded primarily polyiodides and a few Al-containing clusters. Most notable is the remarkable appearance of AlI_4^-, a known closed-shell iodoaluminate anion. HBr and HCl, when introduced into the cluster source's plasma, yielded similar distributions. In no case was this method appropriate for the production of the type of broad distribution of Al-rich clusters necessary for a determination of relative stabilities of Al_nX^- via oxygen etching. In fact, none of the clusters produced in this manner were susceptible to oxygen etching. Likely, excited species exiting the laser-induced plasma were completely reacted with excess HX in the cluster source's nozzle during the cooling phase of their formation. As shown, some larger aluminum halides, such as Al_2I_6, were observed, but tended to incorporate atomic oxygen, likely from trace residual surface oxides on the Al rod. Despite some mass degeneracy issues (ten Al atoms in a cluster have the same mass as two I atoms and one O atom), these peaks were confidently assigned due to the spacings of 16 amu in this mass range.

Tandem reaction experiments, where Al_n^- were first reacted with small amounts of HX added downstream from the LaVa source and then exposed to O_2, did allow for the determination of the relative cluster stabilities. Figure 7 shows the results of these studies for Al_nI^- and Al_nCl^-. Also shown are the results for doubly iodized aluminum clusters. Histograms are used to alleviate visual distractions arising from the presence of bare Al_n^-. Interestingly, in the raw mass spectrometric data, an I^- peak is observed in the tandem reactions featuring HI. Because the peak appears even with no oxygen etching, it is thought to mainly arise due to the closer proximity of the first RGI to the source. In this region of the flow tube, it is far more likely that electrons generated in the cluster source could collide with the reactant gas and

produce I^-. Still, the I^- peak was observed to grow upon introduction of oxygen at the second RGI, indicating that I^- is also a product of the oxygen etching of $Al_nI_x^-$ clusters. Br-containing clusters were not studied via tandem reaction due to the mass degeneracy issues discussed above.

Figure 7(a) shows the magic nature of Al_6I^-, Al_7I^-, $Al_{13}I^-$, and $Al_{15}I^-$. Interestingly, in Fig. 7(b), similar trends are observed; the peaks for $Al_6I_2^-$, $Al_7I_2^-$, $Al_{13}I_2^-$, and $Al_{15}I_2^-$ all grow slightly as a result of the oxygen-etching reaction (while $Al_8I_2^-$ and $Al_9I_2^-$ also appear to grow in Fig. 7(b), they are not considered magic because they do not consistently grow during oxygen etching).

In Fig. 7(c), it is evident that no magic peak occurs for $Al_{13}Cl^-$. However, the peak for $Al_{15}Cl^-$ does grow upon the introduction of oxygen. It is interesting that $n=6$, 7, and 15 should represent magic numbers for both Al_nI^- and Al_nCl^-. For Al_nI^- and $Al_nI_2^-$ $(n>9)$, an odd-even alternation is evident in the reactivity trends. The persistence of this trend is indicative that the addition of I to these clusters does not substantially affect their electronic structures; spin multiplicities have been previously shown[42] to play a role in the odd-even pattern in the relative stabilities of Al_n^-. The initiation of this trend at $n=9$ may be related to the onset of ''metallic'' bonding, as Al clusters in this size range have been observed to feature efficient mixing of *s* and *p* orbitals due to increased coordination number.[37,42]

Interestingly, this trend is not as clear for the Al_nCl^- case. Considering the anomalously high intensities found in the reactant distribution at $n=12$ and 16, simply examining the product peak intensities can be misleading. Looking at the fraction of the initial peak that is depleted, one can find the odd-even alternation for the range $9<n<18$, but again, it is not nearly as apparent as in the iodized clusters. This is likely due to the fact that Al–Cl bonds are stronger and more polar than Al–I bonds. That the nature of the cluster-X interaction depends fundamentally on X makes it even more intriguing that Al_nI^- and Al_nCl^- are both magic at $n=6$, 7, and 15.

V. COMPUTATIONAL RESULTS

A. Reactions

We start by discussing the halogenation of Al_n^- clusters by HX (X=Cl, Br, or I). Our experiments show that the reactivities vary greatly with X, and so it is clear that the halogenation mechanism must be such that it involves the energies of HX. Energetic properties must show whether halogenation proceeds via etching of the bigger clusters or mere attachment of X and removal of H. We shall focus on HI and HCl as they correspond to the opposite limits.

Before we discuss the operative mechanism, we compare our calculated electronic quantities for a variety of molecules to assess the quantitative accuracy of the current studies. Table I contains our calculated bond lengths and atomization energies (AE) for the neutral and anionic AlI, AlCl, AlH, HI, and HCl molecules. For the anionic clusters, the AEs correspond to the fragmentation into the more stable anion and the neutral species. Wherever possible, the known experimental values are included in parentheses for comparison. Note that the calculated values agree quantitatively with experiment to within a few percent. To understand the mechanism for the formation of magic Al_nI clusters, we will focus on the formation of $Al_{13}I^-$. To this end, we start with the ground-state geometries and the atomization energies of neutral and anionic pure Al_n ($n=12$, 13, and 14) clusters. For Al_{13}, the present AE is different from our previously reported value.[22] In our earlier paper, we had used the energy of spherical Al atoms (with fractional occupation of valence orbitals) for the atomic reference energy. The present value, on the other hand, refers to atoms with integral occupation of valence orbitals. For Al_{12}, the ground-state structure shown here was obtained by optimizing from the icosahedral Al_{13}, where a surface atom was missing. For Al_{14}, the ground-state geometry was obtained by optimizing a structure generated by adding an Al atom at a threefold coordinated site of an icosahedral Al_{13}. Note that for the cluster sizes investigated here, it is difficult to carry out an extensive search over all possible geometries. Figure 8 shows the ground-state geometries and Table II contains the AEs and adiabatic electron affinities (AEA). Note that the ground-state geometry of Al_{13}^- is an almost perfect icosahedral structure with a bond length of 2.80 Å between the surface Al sites. We also calculated the ground-state geometries of the neutral and anionic $Al_{13}H$, $Al_{13}I$, and $Al_{13}Cl$ clusters (Fig. 8) by optimizing initial geometries obtained by placing H, Cl, and I atoms at the on-top, bridge, or hollow sites of an Al_{13} icosahedron. Our findings on $Al_{13}H$ are in reasonable agreement with Mañanes *et al.*[43] and Burkart *et al.*[17] The H atom occupies an on-top site for the anion while it occupies a threefold site in case of the neutral cluster. For the neutral $Al_{13}H$, our calculated binding energy of 2.91 eV for a H atom binding to Al_{13} is slightly less than the value of 3.36 eV obtained by Mañanes *et al.*[43] This difference is largely due to the fact that while our calculations are based on a gradient-corrected density functional, the calculations by Mañanes *et al.*[43] use a local spin-density functional, which is known to yield higher binding energies. For the $Al_{13}X^-$ clusters, the AE corresponds to the minimum energy required to fragment into an Al_{13}/Al_{13}^- cluster and an anionic/neutral halogen atom. Note that in all the $Al_{13}X^-$ clusters, the X atom occupies an on-top site. For

TABLE I. Bond length (BL), atomization energy (AE), and electron affinity (EA) of diatomic molecules related to the present studies. For anions, the AE corresponds to the fragmentation into a neutral and the more stable anion.

	Neutral		Anion		
Molecule	BL (Å)	AE (eV)	BL (Å)	AE (eV)	EA (eV)
AlI	2.59 (2.54)	4.01 (3.83)	2.81	1.17	0.46
AlCl	2.17 (2.13)	5.23 (5.30)	2.32	1.80	0.19
AlH	1.68 (1.65)	2.99 (2.95)	1.72	2.75	0.17
HI	1.63 (1.61)	3.49 (3.09)	2.39	0.32	0.14
HCl	1.29 (1.27)	4.64 (4.47)	2.03	0.36	NA

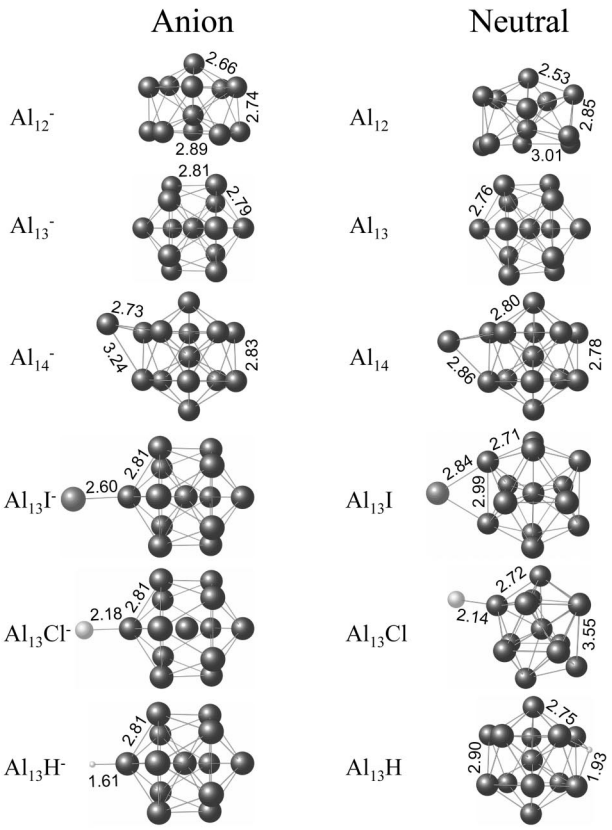

FIG. 8. Ground-state geometries for neutral and anionic Al_n ($n=12$, 13, and 14), $Al_{13}H$, $Al_{13}I$, and $Al_{13}Cl$. Bond lengths are given in angstroms.

X=I and Cl, the Al_{13} unit resembles that of the bare Al_{13}^- cluster. For $Al_{13}I^-$ and $Al_{13}Cl^-$, the calculated AE are 2.46 and 3.29 eV, respectively. As pointed out before, we also carried out supplementary calculations using the GAUSSIAN 98 code to examine the effect of relativistic corrections for I. The ground state corresponds to the halogen atoms occupying the on-top site as in the NRLMOL calculations. Further, the AE values for $Al_{13}I^-$ and $Al_{13}Cl^-$ using the GAUSSIAN 98 code are 2.20 and 3.35 eV, respectively, which are within a few percent of the values obtained using the NRLMOL code, also given are the AEAs.

TABLE II. Atomization energies to break Al_n clusters (to break into n Al atoms), fragmentation energy of the $Al_{13}X$ clusters (to break into the more stable neutral and anionic Al_{13} and X units), and adiabatic electron affinities (AEA) for Al_n and $Al_{13}X$ clusters.

	Atomization/fragmentation energy (eV)		
Cluster	Anion	Neutral	AEA (eV)
Al_{12}	31.86	29.71	2.09
Al_{13}	36.51	33.58	3.35
Al_{14}	38.59	36.63	2.31
$Al_{13}I$	2.46	2.82	2.99
$Al_{13}Cl$	3.29	3.87	3.03
$Al_{13}H$	2.13	2.91	2.57
	(1.7)[a]	(3.4)[a]	(2.0)[a]
		3.36[b]	1.77[b]

[a]For $Al_{13}H$, experimental values are from Burkart *et al.* (Ref. 17).
[b]For $Al_{13}H$, the theoretical values computed by Mañanes *et al.* are given (Ref. 46).

Using the AEs given in Table II, the energy required to remove an Al atom from Al_{14}^- is 2.08 eV, while the energy required to remove an Al atom from Al_{13}^- is 4.65 eV. The large difference in the fragmentation energy is due to the magic nature of Al_{13}^- arising from filled geometric and electronic shells. Now, consider the reaction

$$Al_n^- + HI \rightarrow Al_{n-1}I^- + AlH. \quad (1)$$

For this reaction to be favorable, the sum of the binding energy of I to Al_{n-1}^- and AlH must be greater than the sum of the energy required to remove an Al atom from Al_n^- and the binding energy of HI. For the case of the reaction in Eq. (1), when $n=14$, we must consider that the sum of energies on the right-hand side of the equation is 5.41 eV (2.46 eV+2.95 eV), while the sum on the left-hand side is 5.17 eV (2.08 eV+3.09 eV). (Note that experimental AE for the values are used for HI and AlH molecules, and the calculated values from Table II are used for the Al_{14}^- and $Al_{13}I^-$ clusters.) The reaction is therefore energetically feasible and leads to the formation of $Al_{13}I^-$ from the Al_{14}^- cluster. A similar process starting from Al_{13}^- is, however, prohibited, since the energy required to remove an Al atom from Al_{13}^- alone is 4.65 eV (as opposed to 2.08 eV for Al_{14}^-). In fact, assuming that the binding energy of I to a given Al_n^- cluster is around 2.5 eV (its value for Al_{13}), the HI reaction would eliminate all the Al_n^- clusters for which the energy required to remove an Al atom is less than about 2.4 eV. In practice, the binding energy of Al_n^- clusters to I should be larger for n different from magic species (as the magic sizes are expected to have the lowest reactivity). The above reaction would therefore eliminate all the Al_n^- clusters except the magic sizes and would lead to the formation of $Al_{n-1}I^-$ clusters. Thus, $Al_{13}I^-$ can be easily formed via etching of larger clusters. A similar reaction with HCl and Al_{14}^-, however, is unfavorable by 0.31 eV due to the stronger binding of HCl relative to HI. Thus, $Al_{13}Cl^-$ is not readily formed via etching.

Given the results of experiments, where Al_{13}^- is "selected" via O_2 etching prior to reaction with HI, there must be some mechanism for $Al_{13}I^-$ formation directly from Al_{13}^-. Can $Al_{13}I^-$ form by the dissociative adsorption of HI on Al_{13}^-? To explore this possibility, a HI molecule was placed around Al_{13}^- with the HI bond parallel and perpendicular to one of the edges. When the HI was initially placed away from the edge, it remained intact and formed a weakly bound (1.46 eV) "physisorbed" state. When HI was forced closer to the Al_{13}^-, the HI bond broke, leading to a final state corresponding to an $Al_{13}H$ and I^-. It seems that this channel would generate I^-, which is not observed in the experimental studies performed in the absence of O_2. Still, the reaction data indicates that Al_{13}^- does participate in a reaction with HI, and so it is important to elucidate the mechanism of this reaction. We can again turn to an energetic evaluation of the reactions in order to better understand our results,

$$Al_{13}^- + HI \rightarrow (Al_{13}H)\cdot I^-,$$

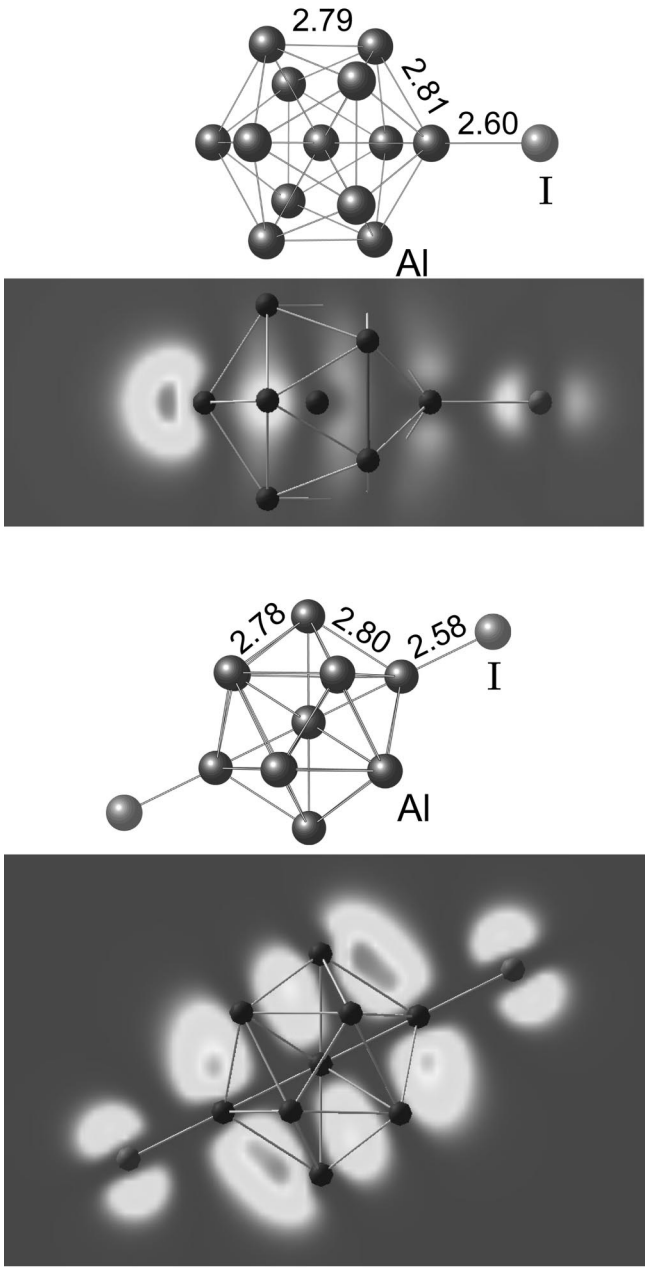

FIG. 9. Ground-state geometry and charge-density map of the HOMO for $Al_{13}I^-$ and $Al_{13}I_2^-$.

$$(Al_{13}H)\cdot I^- + HI \rightarrow Al_{13}I_2^- + H_2, \quad (2)$$

$$(Al_{13}H)\cdot I^- + HI \rightarrow Al_{13}I^- + H_2 + I.$$

Referring to Tables I and II, it is apparent that the weakly bound $Al_{13}HI^-$ cluster will be unstable toward further reactions with HI, thus simultaneously explaining the absence of I^- in the cluster distribution and assuring the validity of the $Al_{13}I^-$ peak assignment. While the secondary reaction, which leads to the formation of $Al_{13}I_2^-$, is more energetically favorable due to the extreme exothermicity of H_2 generation (4.51 eV), it is energetically possible to produce $Al_{13}I^-$ and I. Notably, in this scheme, it might be energetically preferable for the I atom to keep the extra electron, as I's AEA is slightly greater than that calculated for $Al_{13}I$. As no I^- was observed in the reaction of Al_n^- with HI, it seems reasonable to accept that our calculated AEA may be off by 0.07 eV (~2%), and that $Al_{13}I$ does, in fact, have a higher AEA than I. It is also possible that the AEA of Al_{13} plays a more important role here, and that the charge-holding Al cluster moiety simply provides too much of an energetic barrier to allow for the formation of I^-.

We have reported previously on some of the factors that lead to the appearance of $Al_{13}I^-$ as a magic cluster. From Table II, Al_{13} has an AEA of 3.35 eV, compared to the (lower) value of 3.06 eV for I. From the electron affinity alone, it is then clear that Al_{13} would keep most of the electronic charge in $Al_{13}I^-$, as was discussed in our previous publication.[21] Figure 9(a) depicts the charge density of the HOMO in $Al_{13}I^-$; note that most of the charge is, in fact, localized around Al_{13}. A Mulliken population analysis of the total charge indicates a charge of -0.76 around Al_{13} and -0.24 around the I site. The perfect icosahedral structure of the Al_{13} moiety in $Al_{13}I^-$ with Al–Al bond lengths similar to those in Al_{13}^- provides a further testimony that the Al_{13} unit in $Al_{13}I^-$ is an intact Al_{13}^-. We would like to note that the charge on the Al_{13} moiety is not spherically symmetric. This illustrates that part of the bonding can be characterized as a monopole-dipole interaction. The inertness of the $Al_{13}I^-$ can now be easily understood in terms of the formation of Al_{13}^-. As the cluster is exposed to oxygen, the available etching channels involve the formation of AlO, AlO_2, and IO. The resistance of Al_{13}^- to oxygen etching is well documented. The energy needed to remove the I atom from $Al_{13}I^-$ is 2.46 eV, whereas the binding energy of IO is only 2.3 eV. It is thus seen that $Al_{13}I^-$ is energetically stable with respect to oxygen etching.

Experiments show that $Al_{13}Cl^-$ is susceptible to etching by O_2. As Cl has a higher AEA (~3.62 eV) than Al_{13}, the cluster's reactivity can be understood in terms of the effective charge state of the Al_{13} moiety. While it costs 4.65 eV to remove an Al atom from Al_{13}^-, note again that AlCl is bound by 5.23 eV, so that even if $Al_{13}Cl^-$ were to form via the oxygen etching of larger chlorinated clusters, it would be unstable with respect to fragmentation into Al_{12}^- and AlCl. Further, it costs only 3.87 eV to remove an Al atom from a neutral Al_{13}, which would seem to be closer to the true charge state of the Al_{13} moiety in the $Al_{13}Cl^-$ cluster, so that fragmentation or etching would be even easier. As discussed previously,[21] the key to the stability of $Al_{13}X^-$ is in the ability of Al_{13} to remain in its preferred charge state.

Figure 9(c) shows the structure and charge density for $Al_{13}I_2^-$. Like $Al_{13}I^-$, this cluster is characterized by higher charge density on the Al_{13} moiety than on either of the two I atoms at the on-top sites. Mulliken analysis suggests a charge of -0.6 for Al_{13} and -0.2 for each I atom. Here again, it seems that the cluster's resistance to oxygen etching can essentially be explained by the formation of Al_{13}^-.

According to our energetic treatment, the reactions for the neutral species should be somewhat different. Experimental confirmation of these results is precluded by the impossibility of studying neutral species via mass spectrometry (at least without secondary ionization). However, we offer the results here to emphasize the importance of electronic

structure in the present reactions. When neutral Al_{14} is reacted with HI, $Al_{13}H$ and not $Al_{13}I$ should be the favored product according to

$$Al_{14} + HI \rightarrow Al_{13}H + AlI. \quad (3)$$

As can be calculated from the values in Tables I and II, this reaction will be energetically favorable by 0.60 eV. However, the analogous reaction generating $Al_{13}I$ and AlH as products would be energetically unfavorable by 0.37 eV. $Al_{13}H$, however (like $Al_{13}H^-$ in the anion studies), would be unstable to further attack by HI due to the large exothermicity of H_2 production. It is therefore seen that $Al_{13}I$ should ultimately be generated by the etching of neutral Al clusters, even if the pathway is more circuitous than in the anionic case.

VI. DISCUSSION

Energetic treatments of the reactions have shown the favorability of acid-etching pathways. There are two major experimental observations that indicate acid etching, (1) in the previously reported reaction of Al_n^- with HI, the Al_{13}^- peak seems to be continuously populated, and at extremely low concentrations of HI, it has actually been observed to grow very slightly, (2) in the mass spectra for the reaction of Al_n^- with HBr, the closed-shell Jellium species (Al_{13}^-, Al_{23}^-, and Al_{37}^-) emerge as magic peaks, as has been observed in O_2 etching experiments. Still, the reaction of Al_n^- with MeI seeded in O_2 does not mimic the reaction of Al_n^- with HI. This is partially because in the HI case, there is the possibility of I incorporation when the cluster interacts with the etchant. This is obviously impossible with O_2. In addition, the relative etching efficiencies of HI and O_2 are difficult to determine in the present experiments.

It is also interesting to consider that no etching reaction is observed with MeI. We believe that this observation can be explained fairly simply. While the formation of AlH is quite favorable thermodynamically, the same cannot be said for the formation of $AlCH_3$. Trimethylaluminum ($Al(CH_3)_3$) is known to be a stable gas, allowing for the saturative coordination of the aluminum atom. However, an aluminum atom on the surface of an Al_n^- cluster is already coordinated to its neighboring aluminum atoms. Therefore, it is difficult for Me to extract an Al atom from the cluster; rather, as we have described before, it seems more likely that species of the type Al_nCH_3 are generated. In addition, the absence of $Al_nCH_3I^-$ clusters (despite the polarity and polarizability of MeI) in the product distributions from these experiments provides an important corollary to the current experiments with HI. It seems that these species, like their Al_nHI^- analogs, are unstable toward further collisions, leading to the evolution of either Al_nCH_3 and I^- or Al_nI^- and CH_3. There is almost certainly some size dependence in the pathway that is most favorable.

For the reaction between Al_{13}^- and MeI, we previously showed thermodynamically that it would be impossible to generate I^- without a substantial binding energy between the cluster and the methyl group.[18] Here, we revisit this evaluation, including revisions that use the more recent estimate of the EA of Al_{13}.[21]

$Al_{13}^- \rightarrow Al_{13} + e^-$	3.35 eV
$CH_3I \rightarrow C + \frac{3}{2}H_2 + \frac{1}{2}I_2$	−0.14
$\frac{1}{2}I_2 \rightarrow I$	1.03
$I + e^- \rightarrow I^-$	−3.05
$C + \frac{3}{2}H_2 \rightarrow CH_3$	1.42

$$Al_{13}^- + CH_3I \rightarrow Al_{13} + CH_3 + I^- \quad \sim 2.61 \text{ eV}. \quad (4)$$

The new estimate requires a higher binding energy between the cluster and the CH_3 group. By substituting values from Tables I and II into the above evaluation, it is possible to obtain comparable evaluations for each of the reactions discussed here. Assuming no interaction energy between Al_{13}, H, and X^- in each case, the reaction would require 3.39, 3.81, and 4.20 eV for X=I, Br, and Cl, respectively. Clearly, all of the HX reactants would require substantially more interaction energy between the H atom and the Al cluster to generate X^- than is required in the formation of Al_nCH_3 and I^-. It can also be seen that the periodic trend in the energy, which would be required for X^- generation, does not follow the trend in EA. Thus, it is evident that the strength of the H–X bonds plays the determining role in this evaluation.

In contrast to our past work, where we can only estimate cluster-CH_3 interaction energies from the thermodynamic considerations and the presence of I^- in the experiment,[18] for the HX reactions, we have past and present cluster-H bond energies to serve as a guide.[17,42–45] In neutral $Al_{13}H$, the H atom is calculated to be covalently bound to the cluster by a value ranging from ~2.91 (present study) to ~3.36 eV (Ref. 46). As explained above, this interaction does not provide enough energy to allow the generation of X^- (although in the HI case, previously reported values do actually approach the threshold value). It is important to recall that Al_{13}^- is not the only reactant in these experiments. Consider, for example, Al_7, which has an EA of only ~2.04 eV.[42] According to calculations by Kawamura *et al.*, this cluster may be bound to a H atom by ~3.18 eV.[44] The H atom in Al_7H withdraws charge from the aluminum cluster, so that it can resemble the magic Al_7^+ species. Formation of this species would obviously be thermodynamically favorable according to the scheme presented in Eq. (4). Why, then, is no X^- generated by this particular neutralization reaction? Evaluation of EAs and H-binding energies would suggest that several other clusters might engage in reactions generating X^- as well. Where is the X^-?

Pending a detailed theoretical survey of the Al_nX^- series (of particular interest will be the magic $n=6$, 7, and 15 clusters), we offer here a phenomenological treatment of the reactions. Consider again the energies required to break the various H–X bonds. When HI engages a cluster surface, it would be expected to immediately dissociate. HBr and HCl will each be increasingly less inclined to do so. Upon dissociation, or even preceding it, H–Al and Al–X bonds will form. Both types of bonds are stronger than the Al–Al

bonds, and as is evidenced in the O_2 etching experiments, they are less likely to break. Whether oxygen or acid etching is occurring, the etchant will continuously attack Al atoms rather than X atoms.[46] AlH and AlX are shown above to be good leaving groups, and as we have shown, Al_nH (neutral or anionic) clusters may be very susceptible to further attack by HX due to the energetic favorability of evolving H_2. We propose that the majority of acid-etching events are of the following type:

$$Al_n^- + HX \rightarrow Al_{n-2}^- + HAl + AlX. \quad (5)$$

The removal of two Al atoms will then be favored except where magic numbers are involved. For example, large Al_n^- clusters, where n is even, will be expected to lose two Al atoms with each collision with HI until $n=14$, at which point, the reaction is described by Eq. (1). Further, multiply halogenated clusters are believed to evolve via reactions such as that shown in Eq. (2).

VII. CONCLUSIONS

We have provided a comprehensive look at the reactions between aluminum cluster anions and hydrogen halides through both experiment and theory. In all cases, Al_nX^- are produced, and our *ab initio* treatment allowed us to propose reaction pathways in keeping with the data. The reactions described here—primarily acid etching—are shown to be very different from those believed to occur between Al_n^- and MeI, the system in which Al_nX^- clusters were first observed.[18] Thermodynamic considerations show that the reaction outcomes are more dependent on H–X bond strength than AEA, so that the reactivity decreases upon ascension of the periodic table.

We also ascertained the relative stabilities of Al_nI^- and Al_nCl^- via tandem reaction experiments featuring O_2 etching. For Al_nI^-, $Al_nI_2^-$, and Al_nCl^-, $n=6$, 7, and 15 are shown to be particularly resistant to attack by O_2; etching experiments were not performed on the Al_nBr^- clusters, where mass degeneracies make definitive peak assignments impossible. No magic $Al_{13}Cl^-$ peak is observed. We have shown energetically that this cluster will be reluctant to form, and that if formed, it will be highly susceptible to etching.

$Al_{13}X^-$ is only stable when the supermagic Al_{13}^- is bound to a halogen atom of lower EA, allowing it to preserve its favored charge state. The observed stability of $Al_{13}I_2^-$ shows that Al_{13}^- can maintain its geometric and electronic integrity even when interacting with more than one potentially reactive atom; this is very important for the realization of saltlike cluster-assembled materials because it shows that Al_{13} has the potential to mimic a halogen atom in an extended lattice. Taking synthetic advantage of the halogenlike chemistry of Al_{13}, in particular, and the third dimension of the periodic table of elements provided by superatoms in general, will likely lead to many unique opportunities for the synthesis of novel nanostructured materials.

Note in proof. The C_s structure recently reported by Han and Jung [J. Chem. Phys. **121** (2004), and personal communication] for neutral $Al_{13}I$ was also considered in this study. Our NRLMOL calculations found the ground state structure reported here, with its nearly icosahedral AL_{13} moiety, to be very slightly lower in energy.

ACKNOWLEDGMENTS

The authors are grateful to the United States Department of Energy (Grant No. DE-FG02-02ER46009) for financial support of both theory and experiment, and to the United States Air Force Office of Scientific Research (F49620-01-1-0380) for financial support of the acid-etching experiments. S.N.K. and T.M. have enjoyed discussions with N. O. Jones, and D.E.B. and A.W.C. thanks Michele Kimble for support with the experimental apparatus.

[1] W. D. Knight, K. Clemenger, W. A. de Heer, W. A. Saunders, M. Y. Chou, and M. L. Cohen, Phys. Rev. Lett. **52**, 2141 (1984).
[2] R. E. Leuchtner, A. C. Harms, and A. W. Castleman, Jr., J. Chem. Phys. **91**, 2753 (1989); **94**, 1093 (1991); A. C. Harms, R. E. Leuchtner, S. W. Sigsworth, and A. W. Castleman, Jr., J. Am. Chem. Soc. **112**, 5673 (1990).
[3] B. D. Leskiw and A. W. Castleman, Jr., Chem. Phys. Lett. **316**, 31 (2000); B. D. Leskiw, A. W. Castleman, Jr., C. Ashman, and S. N. Khanna, J. Chem. Phys. **114**, 1165 (2001).
[4] S. N. Khanna and P. Jena, Phys. Rev. B **51**, 13705 (1995).
[5] C. Ashman, S. N. Khanna, F. Liu, P. Jena, T. Kaplan, and M. Mostoller, Phys. Rev. B **55**, 15868 (1997).
[6] B. K. Rao, S. N. Khanna, and P. Jena, J. Cluster Sci. **10**, 477 (1999).
[7] J. A. Alonso, M. J. López, L. M. Molina, F. Duque, and A. Mañanes, Nanotechnology **13**, 253 (2002).
[8] A. Schnepf and H. Schnöckel, Angew. Chem., Int. Ed. **41**, 3532 (2002), and references therein.
[9] J. Jia, J.-Z. Wang, X. Liu, Q.-K. Xue, Z.-Q. Li, Y. Kawazoe, and S. B. Zhang, Appl. Phys. Lett. **80**, 3186 (2002).
[10] J. H. Son, Y.-U. Kwon, and O. H. Han, Inorg. Chem. **42**, 4153 (2003), and references therein.
[11] O. C. Thomas, W.-J. Zheng, T. P. Lippa, L.-J. Xu, S. A. Lyapustina, and K. H. Bowen, Jr., J. Chem. Phys. **114**, 9895 (2001).
[12] O. C. Thomas, W. Zheng, and K. H. Bowen, Jr., J. Chem. Phys. **114**, 5514 (2001).
[13] X. Li and L. S. Wang, Phys. Rev. B **65**, 153403 (2002).
[14] H. Kawamata, Y. Negishi, A. Nakajima, and K. Kaya, Chem. Phys. Lett. **337**, 255 (2001).
[15] O. P. Charkin, D. O. Charkin, N. M. Lkimenko, and A. M. Mebel, Chem. Phys. Lett. **365**, 494 (2002).
[16] A. Pramann, A. Nakajima, and K. Kaya, J. Chem. Phys. **115**, 5404 (2001).
[17] S. Burkart, N. Blessing, B. Klipp, J. Müller, G. Ganteför, and G. Seifert, Chem. Phys. Lett. **301**, 546 (1999).
[18] D. E. Bergeron and A. W. Castleman, Jr., Chem. Phys. Lett. **371**, 189 (2003).
[19] D. E. Bergeron and A. W. Castleman, Jr., Int. J. Mass. Spectrom. **230**, 71 (2003).
[20] Al_n^- were first reacted with O_2 to isolate Al_{13}^- and Al_{23}^-. These clusters were then exposed to Mel seeded in He. No appreciable reaction was observed.
[21] D. E. Bergeron, A. W. Castleman, Jr., T. Morisato, and S. N. Khanna, Science **304**, 84 (2004).
[22] S. N. Khanna, B. K. Rao, and P. Jena, Phys. Rev. B **65**, 125105 (2002).
[23] A. W. Castleman, Jr., K. G. Weil, S. W. Sigsworth, R. E. Leuchtner, and R. G. Keesee, J. Chem. Phys. **100**, 995 (1994).
[24] B. L. Upschulte, R. J. Schul, R. Passarella, R. G. Keesee, and A. W. Castleman, Jr., Int. J. Mass Spectrom. Ion Processes **75**, 27 (1987).
[25] M. R. Pederson and K. A. Jackson, Phys. Rev. B **41**, 7453 (1990).
[26] K. A. Jackson and M. R. Pederson, Phys. Rev. B **42**, 3276 (1990).
[27] J. P. Perdew, K. Burke, and M. Irnzerhof, Phys. Rev. Lett. **77**, 3865 (1996).
[28] D. V. Porezag and M. R. Pederson, Phys. Rev. A **60**, 2840 (1999).
[29] M. J. Frisch *et al.*, GAUSSIAN 98, Revision A.7 Gaussian, Inc., Pittsburgh, PA, 1998.
[30] A. D. Becke, J. Chem. Phys. **98**, 5648 (1993).
[31] A. D. Becke, Phys. Rev. A **38**, 3098 (1988).

[32] S. H. Vosko, L. Wilk, and M. Nusair, Can. J. Chem. **58**, 1200 (1980).
[33] C. Lee, W. Yang, and R. G. Parr, Phys. Rev. B **37**, 785 (1988).
[34] B. Miehlich, A. Savin, H. Stoll, and H. Preuss, Chem. Phys. Lett. **157**, 200 (1989).
[35] P. J. Hay and W. R. Wadt, J. Chem. Phys. **82**, 299 (1985).
[36] B. T. Cooper, D. Parent, and S. W. Buckner, Chem. Phys. Lett. **284**, 401 (1998).
[37] X. Li, H. Wu, X.-B. Wang, and L.-S. Wang, Phys. Rev. Lett. **81**, 1909 (1998).
[38] S. H. Yang, D. A. Drabold, J. B. Adams, and A. Sachdev, Phys. Rev. B **47**, 1567 (1993).
[39] L. D. Lloyd, R. L. Johnston, C. Roberts, and T. V. Mortimer-Jones, ChemPhysChem **3**, 408 (2002).
[40] T. P. Martin and J. Diefenbach, J. Am. Chem. Soc. **106**, 623 (1984).
[41] Z. Y. Chen, G. J. Walder, and A. W. Castleman, Jr., Phys. Rev. B **49**, 2739 (1994).
[42] B. K. Rao and P. Jena, J. Chem. Phys. **111**, 1890 (1999).
[43] A. Mañanes, F. Duque, F. Mendez, M. J. Lopez, and J. A. Alonso, J. Chem. Phys. **119**, 5128 (2003).
[44] H. Kawamura, V. Kumar, Q. Sun, and Y. Kawazoe, Phys. Rev. B **65**, 045406 (2001).
[45] S. N. Khanna and P. Jena, Chem. Phys. Lett. **219**, 479 (1994).
[46] This also helps to explain the generation of I^- in the tandem reactions where O_2 etching follows reaction with HI. O_2 will remove Al atoms from an Al_nI^- cluster until only the I^- is left.